Supplemental figure legends

Supplemental Figure S1. Oct-4, nestin and tubulin-β-III expression during differentiation.
(A) Oct4 immunofluorescence (red) in undifferentiated ES cells (top), cells 24 hrs after LIF withdrawal (middle) and in NPC (bottom). DAPI, left; overlay, right.
(B) Nestin immunofluorescence (red) in undifferentiated ES cells (top), cells 24 hrs after LIF withdrawal (middle) and in NPC (bottom). DAPI, left; overlay, right.
(C) TUJ1 immunofluorescence (tubulin-β-III, red) in undifferentiated ES cells (top), cells 24 hrs after LIF withdrawal (middle) and in NPC (bottom). DAPI, left; overlay, right.
(D) Cell counts of Oct4, nestin and TUJ1 positive cells are given as percentage ± stdev.

Supplemental Figure S2. Nuclear area and height in ESC and NPC.
(A) Distribution of the nuclear area in undifferentiated ES cells (red) and neural progenitor cells (NPC) (blue). No significant change was observed ($P > 0.5$).
(B) Distribution of nuclear height in ESC (red) and NPC (blue), estimated indirectly by the Z-stack DAPI thickness using a confocal laser scanning microscope. A decrease from 10.9 ± 2.2 in ESC to 8.4 ± 1.9 in NPC was measured ($P < 0.0001$). Given the 2D nuclear area (A) and the nuclear height (B), we estimate a decrease of ca. 25% in nuclear volume between ESC (~641 ± 126 μm^3) and NPC (~476 ± 107 μm^3) for oval-shaped nuclei ($V = 4\pi abc/3$, where a, b and c are the three radii).

Supplemental Figure S3. Decrease in H3 and H4 acetylation during ES cell neuronal differentiation.
(A) Immunofluoresence of pan-acetylated histone H3 (red) in undifferentiated ES cells (top), cells 24 hrs after withdrawal of LIF (middle) and NPC (bottom). DNA was stained with DAPI (left) and a merged image is shown (right).
(B) Immunofluoresence of pan-acetylated histone H4 (red) in undifferentiated ES cells (top), cells 24 hrs after withdrawal of LIF (middle) and NPC (bottom). DNA was stained with DAPI (left) and a merged image is shown (right).
(C) Western blots of HP1, H3, H2B and H1 in purified nuclei of undifferentiated ES cells, 24 hrs after LIF removal and NPC. The level of these proteins did not change during differentiation.

Supplemental Figure S4. Estimation of exogenous protein levels in transfected cells.
(A) Western blots of HP1, H1, H3 and H2B in purified nuclei of undifferentiated ES cells (left) or NPC (right) transfected with GFP-tagged proteins. In all cases, given the transfection efficiencies (~20%), the levels of the exogenous proteins comprised only a fraction (< ~10%) of the endogenous levels.
(B) Western blots of H1 in $H1^0$-GFP stable cells (left) and $H1^0$cc-GFP stable cells (right).

Supplemental Figure S5. $H1^0$cc constructs bind to chromatin more tightly than do $H1^0$ constructs.
(A) $H1^0$ and $H1^0$cc proteins with and without GFP tags were expressed and purified from *E. coli*.
(B) Oligonucleosomal chromatin substrates were prepared from murine erythroleukemia cells as previously described (Gunjan et al., 2001). An approximately 3-fold excess of individual bacterially-produced proteins was allowed to bind to oligonucleosomes by exchange in 10 mM Tris pH 7.1, 70 mM NaCl for 30 min at 25°C. Aliquots were diluted 10-fold into buffer containing 10 mM Tris pH 7.1 and the indicated amount of NaCl. Following incubation on ice for 20 min, unbound H1 was removed by repeated cycles of dilution and concentration of oligonucleosomes on Centricon YM100 membranes. Bound histones were separated by electrophoresis on 18% Tris-HCl SDS gels (BioRad, Hercules, CA). Representative experiments for $H1^0$ (top) and $H1^0$cc (bottom) are displayed.
(C) Amounts of bound tagged and untagged $H1^0$ and $H1^0$cc fusion proteins as well as endogenous H1 were quantitated by densitometry of Coomasie-stained gels and are expressed as a percentage of the amount bound after extraction with 350 mM NaCl.
(D) Salt extraction of stably expressed $H1^0$ fusion proteins. Nuclei from stable BALB/c 3T3 cell lines expressing $H1^0$-GFP or $H1^0$cc-GFP were extracted with the indicated concentration of KCl as described in Methods. Bound $H1^0$-GFP or $H1^0$cc-GFP remaining in the pellet was extracted by incubation with 1M KCl and quantitated by fluorimetry with a Perkin Elmer model LS50B spectrophotometer (excitation, 488 nm, emission, 507 nm) as previously described (Gunjan et al., 2001).

Supplemental Movie S1. FRAP of H3.3-YFP in wt ES cell. Shown are a total of 12 frames taken at 5 sec intervals. Bleaching was after frame 3. Note immediate recovery at frame 4.

Supplemental Movie S2. FRAP of H3.3-YFP in $HirA^{-/-}$ ES cell. Shown are a total of 12 frames taken at 5 sec intervals. Bleaching was after frame 3.

References

Gunjan, A., Sittman, D. B., and Brown, D. T. (2001). Core histone acetylation is regulated by linker histone stoichiometry in vivo. J Biol Chem *276*, 3635-3640.

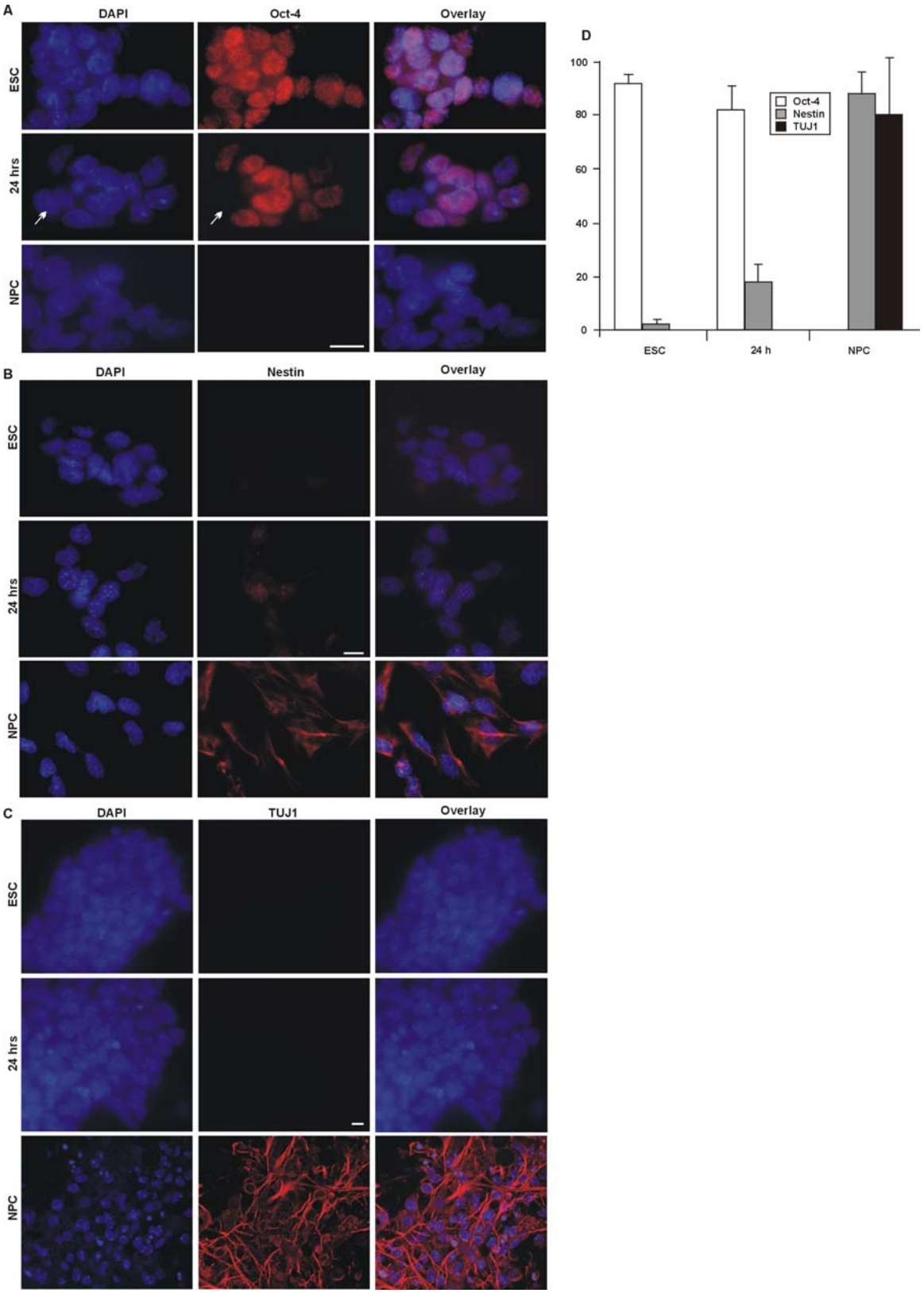

Supplemental Figure S1

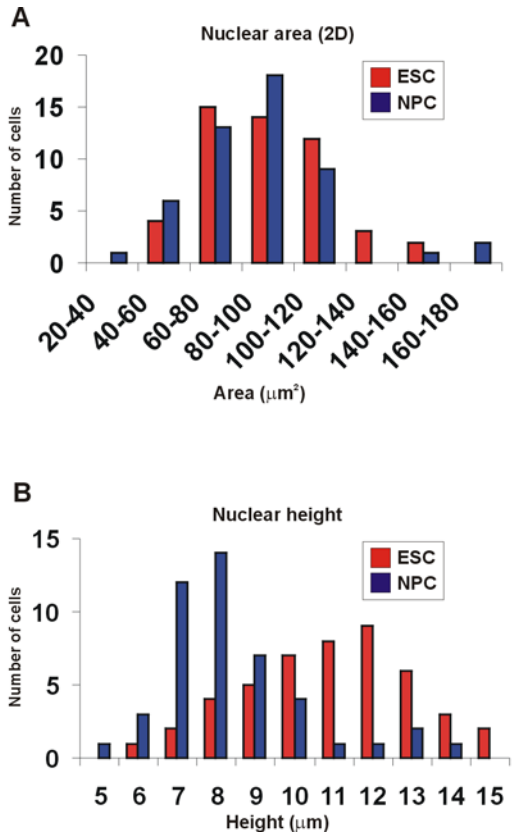

Supplemental Figure S2

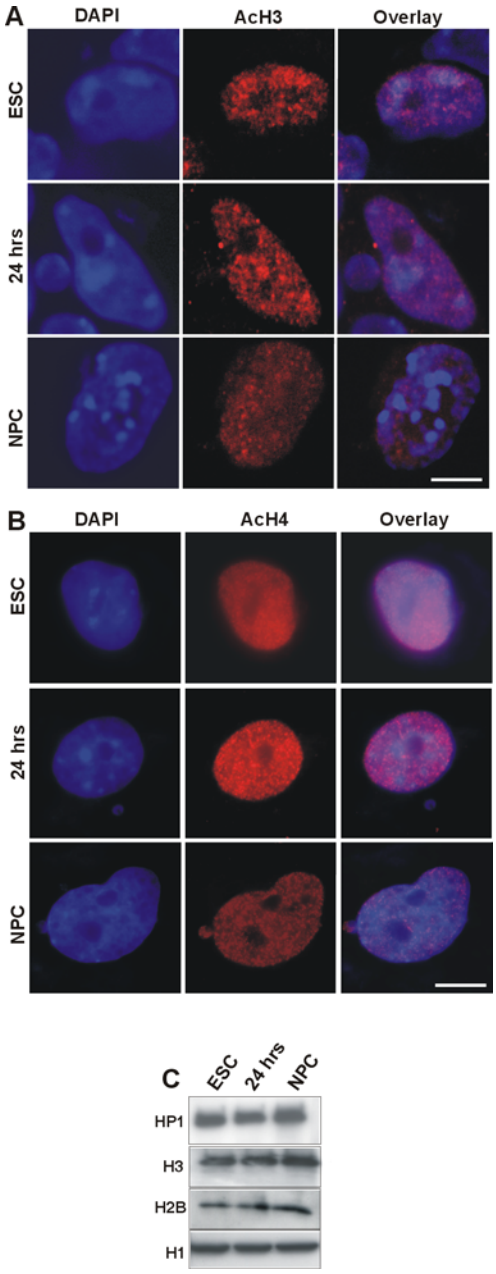

Supplemental Figure S3

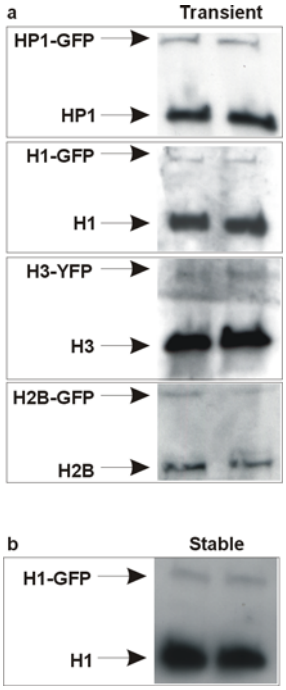

Supplemental Figure S4

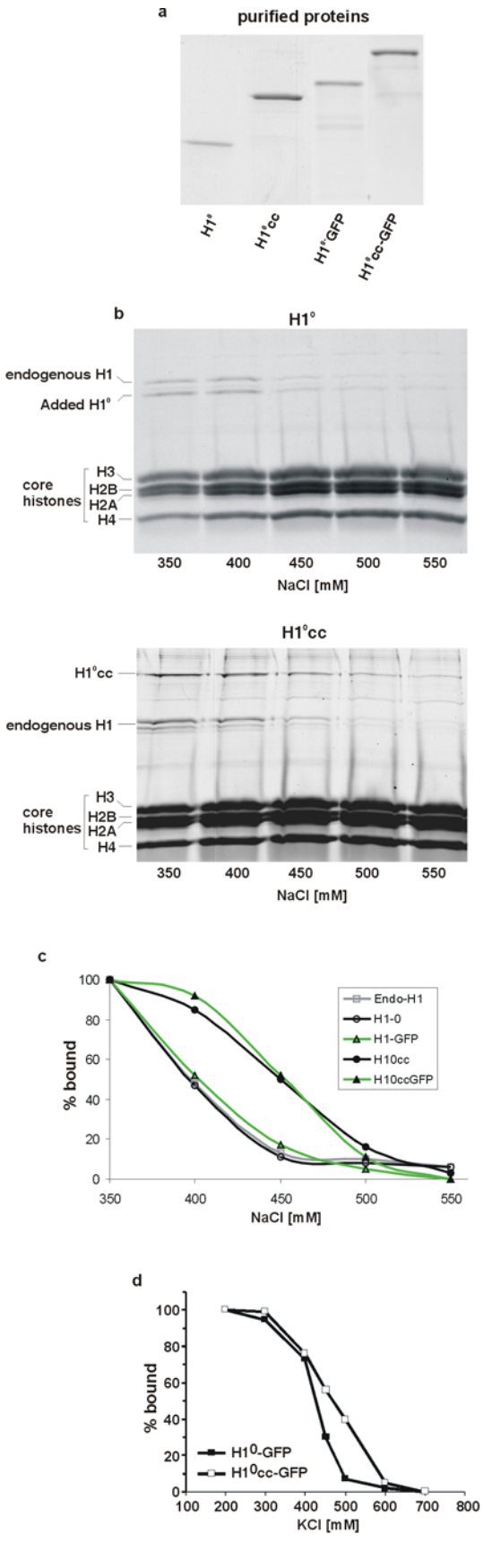

Supplemental Figure S5